AGU PUBLICATIONS

JGR

Journal of Geophysical Research: Space Physics

RESEARCH ARTICLE
10.1002/2016JA023536

Key Points:
- "Zipper-like" magnetosonic waves consist of two-frequency bands with interleaved periodic emissions
- The two bands differ in frequency and intensity but probably originate from one single source
- Zipper-like magnetosonic waves were mainly observed on dawnside to noonside in frequencies between 10 f_{cp} and f_{LHR}.

Correspondence to:
J. Li,
jli@atmos.ucla.edu

Citation:
Li, J., et al. (2017), "Zipper-like" periodic magnetosonic waves: Van Allen Probes, THEMIS, and magnetospheric multiscale observations, *J. Geophys. Res. Space Physics*, *122*, 1600–1610, doi:10.1002/2016JA023536.

Received 28 SEP 2016
Accepted 31 DEC 2016
Accepted article online 7 JAN 2017
Published online 8 FEB 2017

"Zipper-like" periodic magnetosonic waves: Van Allen Probes, THEMIS, and magnetospheric multiscale observations

J. Li[1], J. Bortnik[1], W. Li[1,2], Q. Ma[1], R. M. Thorne[1], C. A. Kletzing[3], W. S. Kurth[3], G. B. Hospodarsky[3], J. Wygant[4], A. Breneman[4], S. Thaller[4], H. O. Funsten[5], D. G. Mitchell[6], J. W. Manweiler[7], R. B. Torbert[8], O. Le Contel[9], R. E. Ergun[10], P.-A. Lindqvist[11], K. Torkar[12], R. Nakamura[12], M. Andriopoulou[12], and C. T. Russell[13]

[1]Department of Atmospheric and Oceanic Sciences, University of California, Los Angeles, California, USA, [2]Center for Space Physics, Boston University, Boston, Massachusetts, USA, [3]Department of Physics and Astronomy, University of Iowa, Iowa City, Iowa, USA, [4]School of Physics and Astronomy, University of Minnesota, Minneapolis, Minnesota, USA, [5]Los Alamos National Laboratory, Los Alamos, New Mexico, USA, [6]Space Department, The Johns Hopkins University Applied Physics Laboratory, Laurel, Maryland, USA, [7]Fundamental Technologies LLC, Lawrence, Kansas, USA, [8]Institute for the Study of Earth, Oceans, and Space, University of New Hampshire, Durham, New Hampshire, USA, [9]Laboratoire de Physique des Plasmas (UMR7648), CNRS/Ecole Polytechnique/UPMC/Université Paris-Sud 11/Observatoire de Paris, Palaiseau, France, [10]Laboratory of Atmospheric and Space Physics, University of Colorado Boulder, Boulder, Colorado, USA, [11]Royal Institute of Technology, Stockholm, Sweden, [12]Space Research Institute, Austrian Academy of Sciences, Graz, Austria, [13]Department of Earth, Planetary and Space Sciences and Institute of Geophysics and Planetary Physics, University of California, Los Angeles, California, USA

Abstract An interesting form of "zipper-like" magnetosonic waves consisting of two bands of interleaved periodic rising-tone spectra was newly observed by the Van Allen Probes, the Time History of Events and Macroscale Interactions during Substorms (THEMIS), and the Magnetospheric Multiscale (MMS) missions. The two discrete bands are distinct in frequency and intensity; however, they maintain the same periodicity which varies in space and time, suggesting that they possibly originate from one single source intrinsically. In one event, the zipper-like magnetosonic waves exhibit the same periodicity as a constant-frequency magnetosonic wave and an electrostatic emission, but the modulation comes from neither density fluctuations nor ULF waves. A statistical survey based on 3.5 years of multisatellite observations shows that zipper-like magnetosonic waves mainly occur on the dawnside to noonside, in a frequency range between 10 f_{cp} and f_{LHR}. The zipper-like magnetosonic waves may provide a new clue to nonlinear excitation or modulation process, while its cause still remains to be fully understood.

1. Introduction

Fast magnetosonic (MS) waves, also known as "equatorial noises" due to their equatorial confinement [*Russell et al.*, 1970; *Santolík et al.*, 2002], are ubiquitously observed in Earth's magnetosphere both inside and outside the plasmapause [*Meredith et al.*, 2008; *Ma et al.*, 2013, 2015; *Hrbáčková et al.*, 2015]. They are nearly linearly polarized and perpendicularly propagating electromagnetic waves and are usually observed in a frequency range between the proton gyrofrequency (f_{cp}) and the lower hybrid frequency (f_{LHR}). It is believed from theory and confirmed by observations that MS waves are generated by energetic proton ring distributions [e.g., *Horne et al.*, 2000; *Chen et al.*, 2010, 2011; *Ma et al.*, 2014a]. Recently, MS waves were found to be capable of creating radiation belt electron butterfly distributions [*Ma et al.*, 2015; *Li et al.*, 2016a, 2016b] via Landau resonance [*Horne et al.*, 2007], while *Maldonado* et al. [2016] proposed that bounce resonance also plays a role.

The renewed interest in MS waves is also attributed to their fascinating wave structures. MS waves occurring at harmonics of f_{cp} have been observed by several spacecraft [e.g., *Perraut et al.*, 1982; *Gurnett*, 1976; *Balikhin et al.*, 2015; *Li et al.*, 2016a], and the harmonic structure is found to be consistent with an instability caused by the proton ring distribution [*Chen*, 2015; *Chen et al.*, 2016]. Recently, observations from Time History of Events and Macroscale Interactions during Substorms (THEMIS) satellites and Van Allen Probes showed that magnetosonic waves sometimes exhibit periodic rising-tone features with a repetition period of a few minutes [*Fu et al.*, 2014; *Boardsen et al.*, 2014], but the modulation is not associated with density fluctuation or ultralow frequency (ULF) waves in those case studies. A more recent study using long duration waveform magnetic field data measured by the Cluster satellites showed that each single element of the periodic rising-tone emission consists of multiple harmonic structures [*Němec et al.*, 2015]. The statistical results by *Němec et al.* [2015] also show that compressional ULF waves are identified in about 46% of the rising-tone magnetosonic wave events, and their periods are mostly near twice of the magnetosonic wave recurring period.

This paper reports a new wave structure observed in the highly resolved magnetosonic wave spectrogram that we call “zipper-like” structure, which consists of two series of periodic rising-tone elements that interleave together with spectral features like a zipper. The wave and particle data set used in this study is described in section 2. Three events are investigated to study the features of the zipper-like MS waves and their possible modulation sources in section 3. In section 4, we present our statistical survey of the zipper-like structures and discuss their preferential occurrence regions. Our conclusions are drawn in section 5.

2. Data Set

The Magnetospheric Multiscale (MMS) mission, a constellation of four identical satellites with separations down to 10 km, is designed for investigating the magnetic reconnection process at the dayside magnetopause and in the magnetotail [*Burch et al.*, 2015; *Fuselier* et al., 2016]. During the first phase, they travel in a 1.2 $R_E \times 12$ R_E orbit to enable dayside measurements. The FIELDS instrumentation suite [*Torbert et al.*, 2014] provides comprehensive high time-resolution DC magnetic and electric field and wave measurements, including a fluxgate magnetometer [*Russell et al.*, 2014] which measures the magnetic field with a cadence of 128 samples/s, a triaxial search coil magnetometer (SCM) [*Le Contel et al.*, 2014] which measures magnetic spectrum over 1–6000 Hz, a spin plane double probe (SDP) [*Lindqvist* et al., 2016] and a Axial Double Probe (ADP) [*Ergun et al.*, 2014] that measure the DC to ~100 kHz electric fields in the spin plane and along the spin axis, respectively. The magnetic and electric waveform measured by SCM, SDP, and ADP are processed inside the digital signal processor (DSP), producing 2 s resolution fast mode wave spectra in region of interest and 16 s resolution slow mode wave spectra in the inner magnetosphere including the radiation belt region. The SDP instrument also measures the spacecraft potential and thus provides an estimate of the ambient plasma density, but at times the Active Space Potential Control (ASPOC) [*Torkar et al.*, 2014] controls the spacecraft potential, and thus, the estimation of the ambient plasma density requires an additional analysis [*Andriopoulou et al.*, 2015; 2016].

The twin Van Allen Probes were designed to measure the evolution of energetic particle dynamics and wave evolutions in Earth’s radiation belts [*Mauk et al.*, 2013]. They travel in an orbit of 1.1 $R_E \times 5.8$ R_E with 10° inclination angle. The Electric and Magnetic Field Instruments Suite and Integrated Science (EMFISIS) [*Kletzing et al.*, 2013] Waves instrument provides electric spectral measurements in a frequency range of 10 Hz–400 kHz and magnetic spectral measurements over 10 Hz–12 kHz, both at a cadence of 6 s. The fluxgate magnetometer (MAG) instrument provides magnetic field measurements with 64 Hz sampling rate, and the Electric Field and Waves (EFW) [*Wygant et al.*, 2013] measures the electric field and spacecraft potential from which the plasma density can be calculated. The Helium Oxygen Proton Electron (HOPE) [*Funsten et al.*, 2013] instrument provides proton flux measurements in an energy range of 1 eV–40 keV, and the Radiation Belt Storm Probes Ion Composition Experiment (RBSPICE) [*Mitchell et al.*, 2013] instrument measures 8–600 keV proton fluxes. In this paper, we also used THEMIS satellites measurements [*Angelopoulos*, 2008] including their search coil magnetometer (SCM) [*Roux et al.*, 2008; *Le Contel et al.*, 2008] and Electric Field Instrument (EFI) [*Bonnell et al.*, 2008].

3. Observations

3.1. Case 1

Figure 1 shows the wave measurements by MMS-2 in the inner magnetosphere during 21:00–22:30 UT on 13 November 2015. The *AE* index (Figure 1a) indicates a few moderate substorm injection events occurred ~12 h preceding the time of wave observation which is marked green. The *SYM-H* index (Figure 1b) reached a minimum of −48 nT at ~6 h before the wave observations, indicating a moderate geomagnetic storm. The plasma density, shown in Figure 1c, is computed from the spacecraft potential measurement following the procedure described by *Andriopoulou et al.*, [2016]. This procedure works well in the plasmatrough region [*Pedersen et al.*, 2008; *Lybekk et al.,* 2012], but the uncertainty is higher in the plasmasphere because of additional assumptions including the ambient electron temperature. This is different from the procedure applied

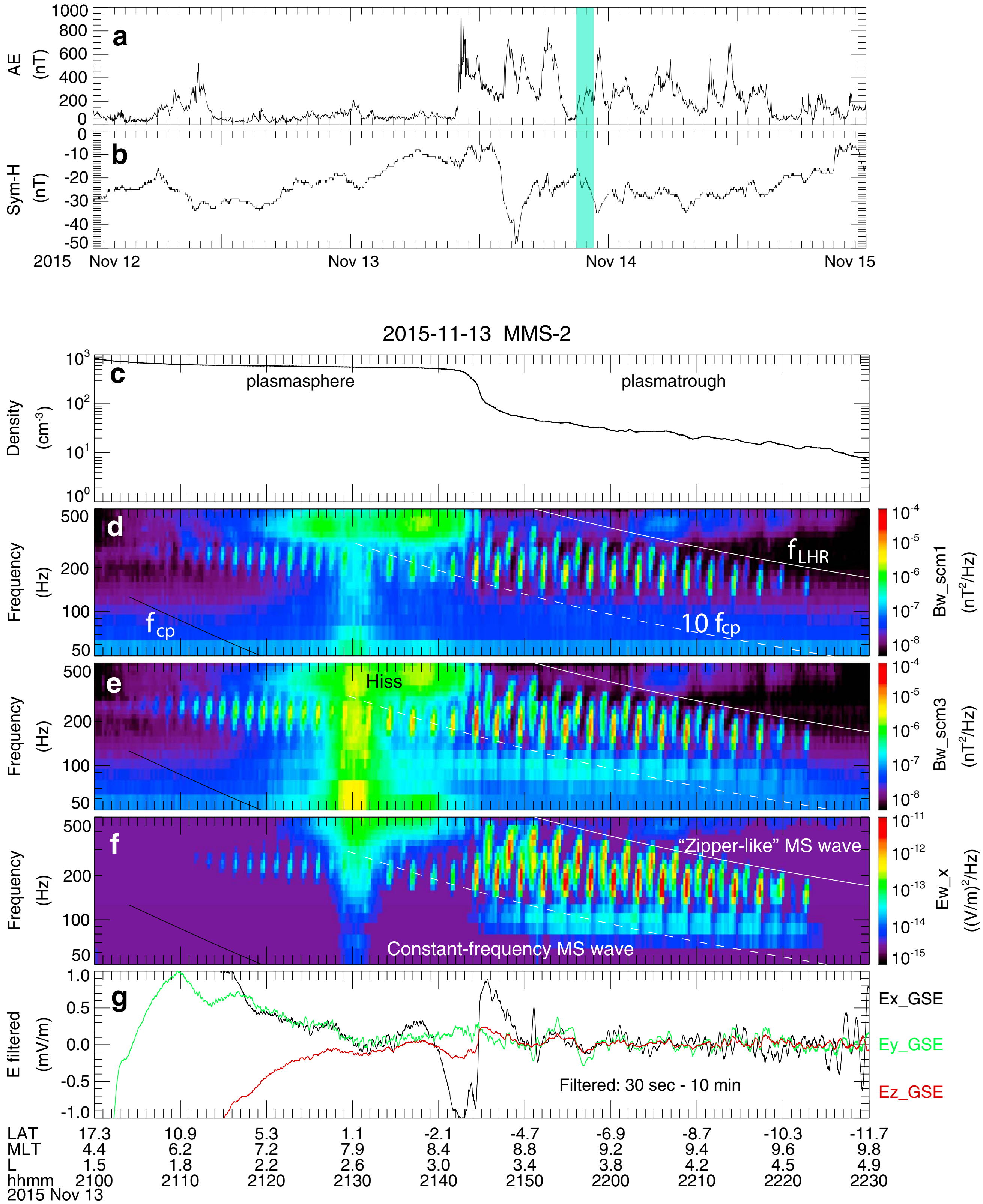

Figure 1. The (a) *AE* index and (b) *SYM-H* index variation during 12–15 November 2015. The green area marks the time of MMS-2 measurements shown below. (c) The plasma density estimated from the spacecraft potential controlled by the ASPOC instrument. The DSP processed wave magnetic spectrum (d) measured by scm1 in the spin plane and (e) that measured by scm3 along the spin axis, overplotted with f_{LHR}, $f_{LHR}/2$, and f_{cp}. (f) The wave electric spectrum in the spin plane measured by SDP. (g) The electric field vector in GSE coordinate system filtered between 30 s and 10 min.

to low Earth orbiting missions in high plasma density environment [e.g., *Fu et al*., 2010a, 2010b]. Despite those uncertainties, the derived density clearly indicates a plasmapause crossing at 21:45 UT at $L = 3.2$.

Figures 1d and 1e show wave magnetic spectrum measured in the spin plane (roughly representing the perpendicular component with regard to the ambient magnetic field) and along the spin axis (roughly representing the parallel component), respectively, and Figure 1f shows wave electric spectrum measured in the spin plane. Structureless hiss emissions were observed inside the plasmasphere over ~300–500 Hz, followed by an observation of two bands of periodic rising-tone MS waves mostly outside the plasmapause. Although the MMS slow mode spectrum measurements do not provide polarization properties, the magnetosonic waves can be identified from their frequency range between f_{cp} and f_{LHR}, their latitudinal confinement of ~10°, and the dominant parallel wave magnetic component compared with the perpendicular component. Both the lower frequency and the higher-frequency sequences of MS waves have a periodicity of ~2.7 min outside the plasmapause. They appear to "gear" together like a zipper, and at a higher L shell of $L = 4.5$ they merge into the same frequency range. Hereafter, we name this kind of emission zipper-like MS waves. The lower frequency band exhibits a larger intensity, and penetrates into the plasmasphere where its periodicity becomes ~1.4 min, while the high-frequency band gradually diminishes in amplitude inside the plasmasphere. The zipper-like MS waves in the plasmatrough were likely to be locally excited, because the higher-frequency band followed the f_{LHR} line, while the periodic MS waves inside the plasmasphere probably originated from a distant source at larger L shell, as MS waves can propagate perpendicularly across magnetic field lines [*Chen and Thorne*, 2012; *Ma et al*., 2014a, 2014b] while keeping their wave frequencies unchanged. Below the frequency of the zipper-like MS waves, a constant-frequency wave is observed over 60–130 Hz, which is also identified as MS wave by its frequency range and dominant parallel wave magnetic component. The constant-frequency feature suggests that they were possibly from a relatively stable source.

Figure 1g depicts the electric field measurements filtered between 30 s and 10 min, which show that those zipper-like MS waves, as well as the periodic constant-frequency MS waves, were not modulated by ULF waves. The magnetic field measurement did not show discernible modulation either and is therefore not presented in this paper. The zipper-like emissions were also not correlated with density variations (Figure 1c), even if we subtracted the trend from the density plot shown in Figure 1c. Note that the 60–130 Hz constant-frequency MS wave is modulated with the same periodicity as the lower frequency band zipper-like MS waves, but the cause of modulation is unclear. The interspacecraft distance of the 4 MMS satellites was about 10 km, which is almost equivalent to the estimated magnetosonic wavelength (~10 km) at 300 Hz based on cold plasma theory. This is probably why the four spacecraft measured almost the same waves, and hence, the observations from the other three satellites are not shown in this paper.

3.2. Case 2

Whether the two bands of the zipper-like MS waves originated from a single source or two sources is unclear in the above case, and analyses of more case studies would be required to address this question. Figure 2 presents a Van Allen Probe observation of zipper-like MS waves during 08:30–10:30 UT on 18 September 2012, which was a relatively geomagnetically quiet day as indicated by the *AE* and *SYM-H* indices in Figures 2a–2b. Figure 2c shows the f_{UHR} measurements from which the plasma density can be calculated, and consequently, the plasmasphere is identified and labeled on top of Figure 2c. From the wave magnetic and electric spectrum measurements shown in Figures 2d and 2e, respectively, we found a constant-frequency MS wave in 30–100 Hz range outside the plasmapause during ~08:30–09:00 UT. Above the frequency of this band, a periodic zipper-like MS wave was observed. The MS waves can be identified from their frequency range generally between f_{cp} and f_{LHR} and characteristic wave normal angles close to 90° (Figure 2f). The ellipticity of those zipper-like MS waves was not clearly close to 0 (Figure 2g), probably because the planarity of those zipper-like MS waves was about 0.5 (Figure 2h), indicating that the assumption of single plane wave is not well fulfilled [*Němec et al*., 2013]. In contrast, the constant-frequency MS waves have planarity well above 0.8, indicating that they were almost single plane waves at each frequency, and hence, their ellipticity was clearly close to 0. During 08:30–09:00 UT the periodic MS waves alternated between a weak one and a relatively intense one, while during 09:00–09:45 UT the waves alternated between a high-frequency one and a low-frequency one.

The intensity of these zipper-like MS waves was seen to increase with decreasing L shells and their frequency follows the f_{LHR} line, suggesting they were either locally generated or outward propagating. In contrast, the intensity of the constant-frequency MS waves in 30–100 Hz range decreases with decreasing L shells,

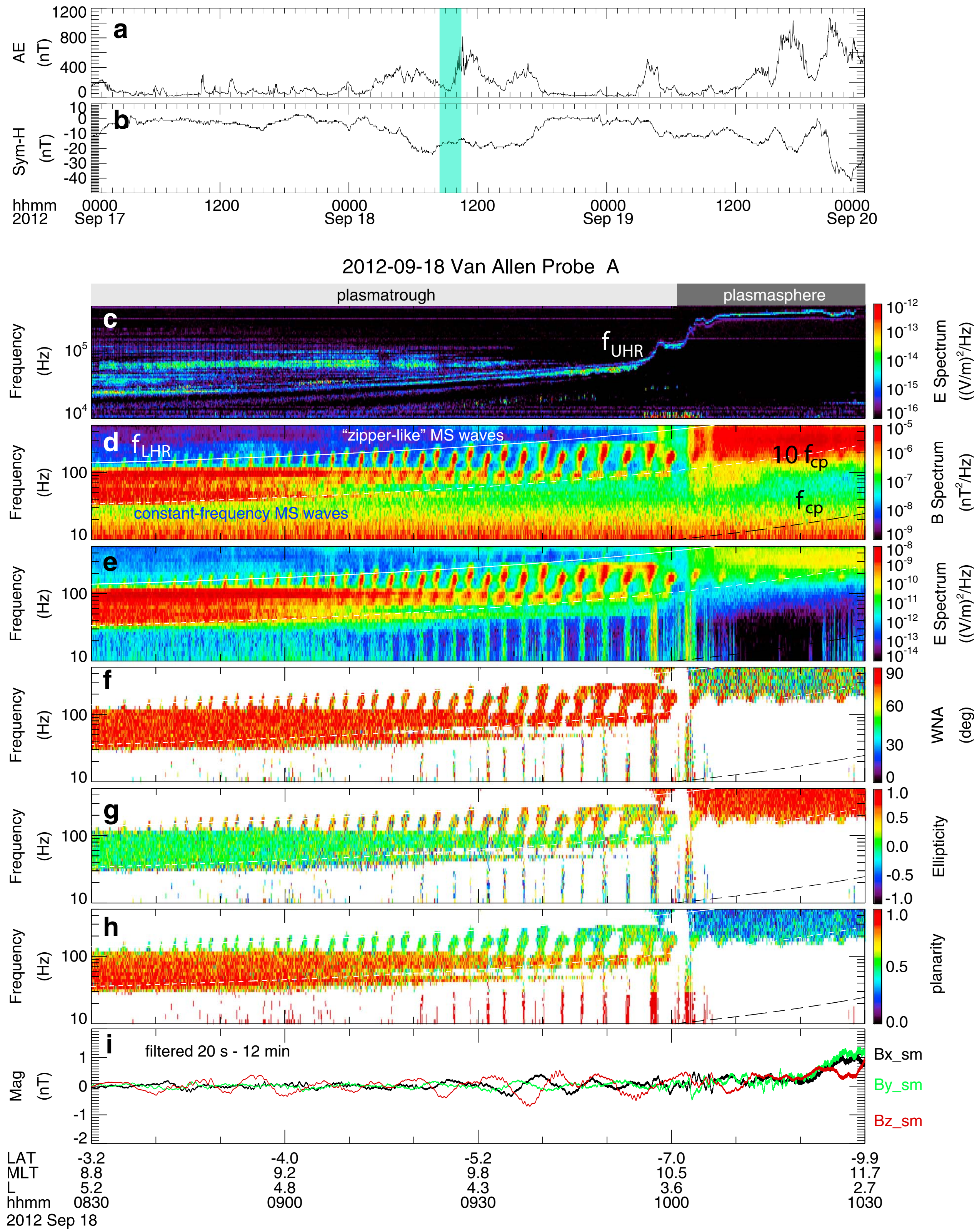

Figure 2. (a) The *AE* index and (b) *SYM-H* index variation during 17–20 September 2012, and the green area marks the time 08:30–10:30 UT on 18 September 2012, corresponding to Van Allen Probe A observations shown below. (c) The wave electric spectrum over a frequency range of 10–500 kHz, overplotted with the f_{UHR} measurement. (d) Wave magnetic spectrum, (e) wave electric spectrum, (f) wave normal angle, (g) wave ellipticity, and (h) wave planarity measurements over a frequency range of 10–500 Hz, overplotted with f_{LHR}, $f_{LHR}/2$, and f_{cp}. (i) The magnetic field fluctuations in SM coordinates filtered between 20 s and 12 min.

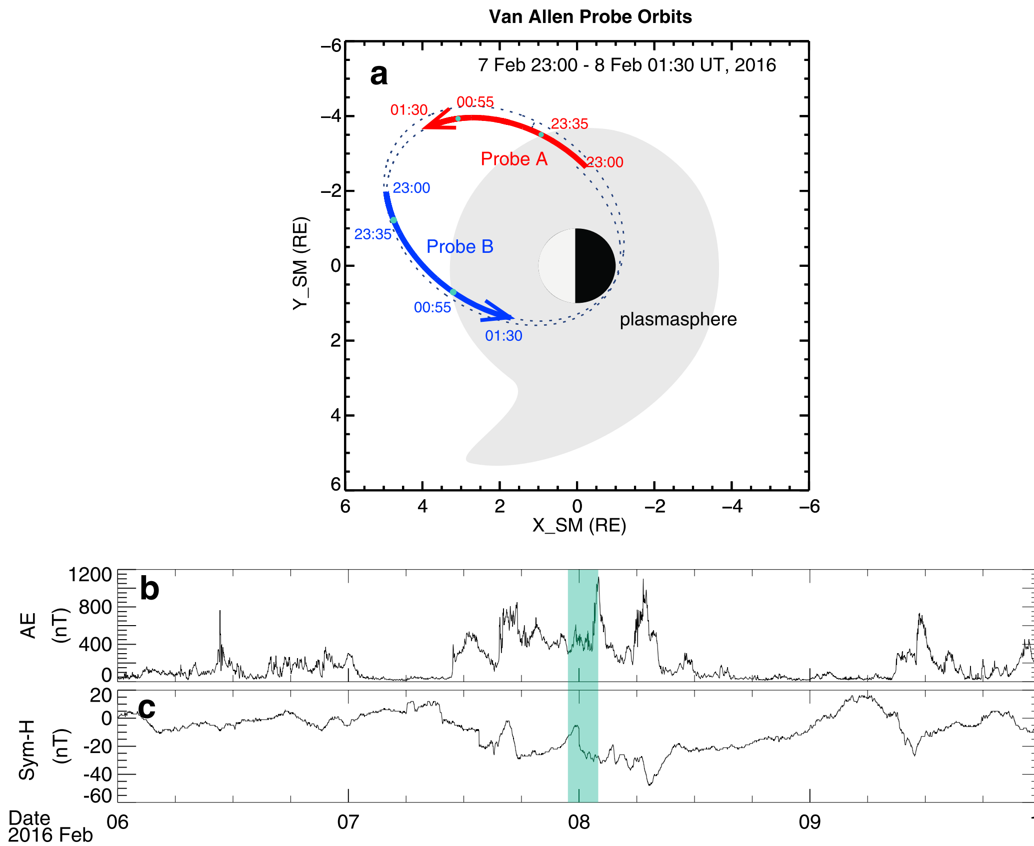

Figure 3. (a) The Van Allen Probes orbits with respect to the plasmasphere from 23:00 UT on 7 February to 01:30 UT on 8 February, 2016. (b and c) The *AE* index and the *SYM-H* index during 6–9 February 2016. The green marks the time periods of Van Allen Probe observations shown in Figure 4.

indicating that they were probably propagating inward from higher L shells. The periodicity of the zipper-like MS waves increased gradually when the satellite traveled to lower L shells. During 08:30–09:00 UT when the probe was at $L = 5.2–4.8$, the periodicity was 2 min, while during 09:30–10:00 UT when the probe was at $L = 4.3–3.6$, the periodicity became 3 min. Since MS waves in the plasmatrough propagate predominantly in the azimuthal direction [*Němec et al.*, 2013], their periodicity change could possibly be due to L shell dependence of the modulation source. An interesting phenomenon is that the constant-frequency band MS wave gradually developed into a discrete one with the same periodicity as the zipper-like MS wave after 09:15 UT, similar to the MMS observations in case 1. It is interesting to note that several electrostatic emissions below 30 Hz were observed with the same repetition period as the zipper-like structures. This suggests that the two bands of those zipper-like MS waves were probably an intrinsic feature at the origin, but not likely a coincidence of mixed two bands merged from different sources. The magnetometer measurement filtered in a periodicity range between 20 s and 12 min, displayed in Figure 2h, shows no discernible ~2–3 min modulations to the zipper-like MS waves. This is consistent with the reports of rising-tone MS waves [*Fu et al.*, 2014; *Boardsen et al.*, 2014]. We note that this event was recorded only 18 days after the launch of Van Allen Probes, and we did not have a chance to examine the in situ proton measurements by HOPE and RBSPICE since they had not started routinely measurements yet.

3.3. Case 3

From case 2 we see that the periodicity of the zipper-like MS waves varied along the satellite orbit. However, any single satellite cannot distinguish spatial variation from temporal variation, while multisatellite measurements may provide more clues of spatiotemporal variations. In the third case, the two Van Allen Probes were separated in magnetic local time (MLT) by at least 3.85 h during the 2.5 h starting from 23:00 UT on 7 February 2016, and their orbits in the solar magnetic (SM) coordinate are displayed in Figure 3a. This event occurred

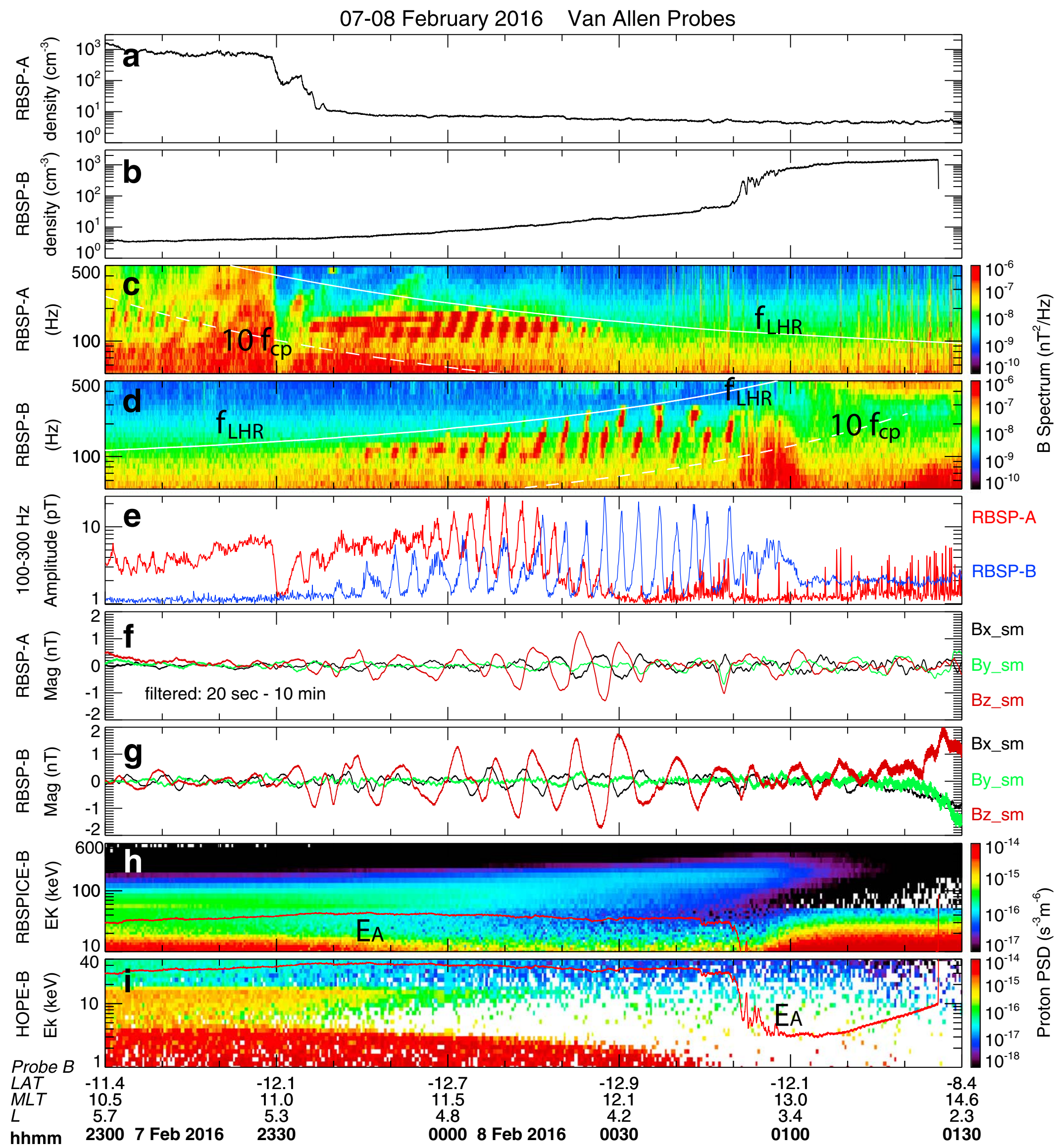

Figure 4. (a and b) The ambient plasma density measured from 23:00 UT on 7 February to 01:30 UT on 8 February 2016 by Van Allen Probes A and B, respectively. (c and d) The wave magnetic spectrum measured over a frequency range of 50–500 Hz by two probes, respectively, overplotted with f_{LHR} and $f_{LHR}/2$. (e) The integrated wave magnetic amplitudes over a frequency range 100–300 Hz measured by both probes, respectively. (f and g) The magnetic field vector components filtered between 20 s and 10 min measured by both probes, respectively. (h) The proton PSD measured along probe B orbit over an energy range of 10–600 keV by the RBSPICE instrument, and (i) that measured over an energy range of 1–50 keV by the HOPE instrument, overplotted with local Alfvén energy.

during the main phase of a geomagnetic storm and was followed by a few injections (Figures 3b and 3c). During the period from 23:30 UT on 7 February to 00:30 UT on 8 February, both probes were outside the plasmasphere, as demonstrated by density measurements in Figures 4a and 4b, and they both observed periodic rising-tone MS waves simultaneously, as shown in wave magnetic spectra measurements in Figures 4c and 4d. However, those rising-tone MS waves at the locations of the two probes had notably different reoccurring periods, clearly indicating that they were originated from difference sources. Figure 4e displays the wave amplitudes integrated over 100–300 Hz measured by both probes, and the wave periodicity observed by probe B (~3.6 min) is longer than that observed by probe A (~3 min). Although the two probes were separated by ~5 R_E in distance, they detected a very similar compressional ULF wave, which had a B_z dominant fluctuation with a period of about 7–8 min (Figures 4f and 4g). This supports the previously suggested scenario that the periodic MS emissions were not modulated by ULF waves [*Fu et al.*, 2014; *Boardsen et al.*, 2014].

During the period of 00:30–00:50 UT on 8 February, such rising-tone emissions split and developed into zipper-like MS waves with a higher-frequency band (~0.5 $f_{\text{LHR}} - f_{\text{LHR}}$) and a lower frequency band (~10 $f_{\text{cp}} - 0.5\ f_{\text{LHR}}$) at the location of probe B. Figure 4h shows the 90° pitch angle proton phase space density (PSD) in an energy range of 10–600 keV measured by the RBSPICE instrument onboard Van Allen Probe B, and Figure 4i shows the 90° pitch angle proton PSD measured in an energy range of 1–40 keV by the HOPE instrument overplotted with the Alfvén energy $E_A = m_p v_A^2/2$, where m_{p} represents proton mass and v_{A} is the Alfvén speed. We note that there is a factor of 1 to 3 difference between the proton fluxes measured by the HOPE and that by the RBSPICE instrument [*Kistler et al.*, 2016], despite that the RBSPICE proton fluxes at low energies contain contaminations from O^+. A positive PSD gradient around the Alfvén energy is observable at the time when probe B observed MS waves, and the ring current energy E_{RC}, identified by the PSD peak, was higher than E_{A} after 00:20 UT on 8 February when the zipper-like MS waves were observed by probe B. Assuming that the waves were at the source region (while they may also propagate from other locations [*Horne et al.*, 2000]), the particle measurements indicate that the generation of this zipper-like MS wave is different from linear excitation theory, which shows that higher-frequency MS waves are preferentially excited when E_{A} is higher than E_{RC}, whereas the lower frequency MS waves are excited when E_{A} is slightly lower than E_{RC} [*Ma et al.*, 2014a]. Besides, the periodic recurring indicates a potential nonlinear process [*Fu et al.*, 2014]. The zipper-like MS waves were not observed after 00:50 UT when probe B traveled into the plasmasphere and the Alfvén energy became significantly lower.

4. Discussion

In all three events investigated in this paper, the zipper-like MS waves were observed during geomagnetically disturbed times with substorm injections and were generally in a frequency range between ~10 f_{cp} and f_{LHR} and mostly outside of the plasmapause. This frequency range is possibly associated with the wave occurrence locations, as a statistical investigation based on Van Allen Probe observations from September 2012 to August 2014 shows that the MS waves at $L > 4$, regardless of their structures, were mostly observed at frequencies above 10 f_{cp} [*Boardsen et al.*, 2016]. The zipper-like MS waves were not observed at higher L shells in all three cases above, possibly because they are damped by suprathemal electrons when their frequencies approach the local f_{LHR} and their refractive indices approach infinity. These three zipper-like MS waves were not related to electron butterfly distributions (not shown in this paper), probably because the time-averaged wave intensities were too small (~10 pT, although the peak may reach 50 pT), while the MS waves that were reported to have created butterfly distributions within one day were at least 240 pT [*Li et al.*, 2016a, 2016b; *Maldonado* et al., 2016].

A statistical study has been performed on the occurrence of rising-tone MS waves and the zipper-like MS waves during the Van Allen Probe era from September 2012 to April 2016. THEMIS A, THEMIS D, THEMIS E measurements during this era and MMS measurements from September 2015 to April 2016 are also included into this statistical study (only one MMS satellite is used because the four probes were so close together that they always measured the same waves in the inner magnetosphere). A total of 308 clearly identified rising-tone MS wave events with duration longer than 10 min were recorded by these satellites (269 from Van Allen Probes, 26 from THEMIS, and 13 from MMS). Figure 5a shows the spacecraft orbits in the equatorial plane of SM coordinate system where rising-tone MS waves were observed by any of those satellites. The rising-tone MS waves were mostly observed on the dawnside, dayside, and duskside in a radial range between 1.2 R_E and 6 R_E, while there are also a few observations on the nightside at $L < 4$, possibly due to azimuthal propagation from the dayside. This result is consistent with the distributions of all the MS waves [*Ma et al.*, 2013, 2015]. A total of 21 zipper-like MS waves were identified (17 from Van Allen Probes, 1 from THEMIS, and 3 from MMS), and all of these emissions were associated with substorm injections. Their locations are illustrated in Figure 5b, showing that they are observed mainly on the dawnside to noonside (6–13 MLT). However, we note that measurements from more satellites over a longer period are needed to construct a more precise global distribution of zipper-like waves. Since the number of identified rising-tone MS waves is more than the number of zipper-like waves

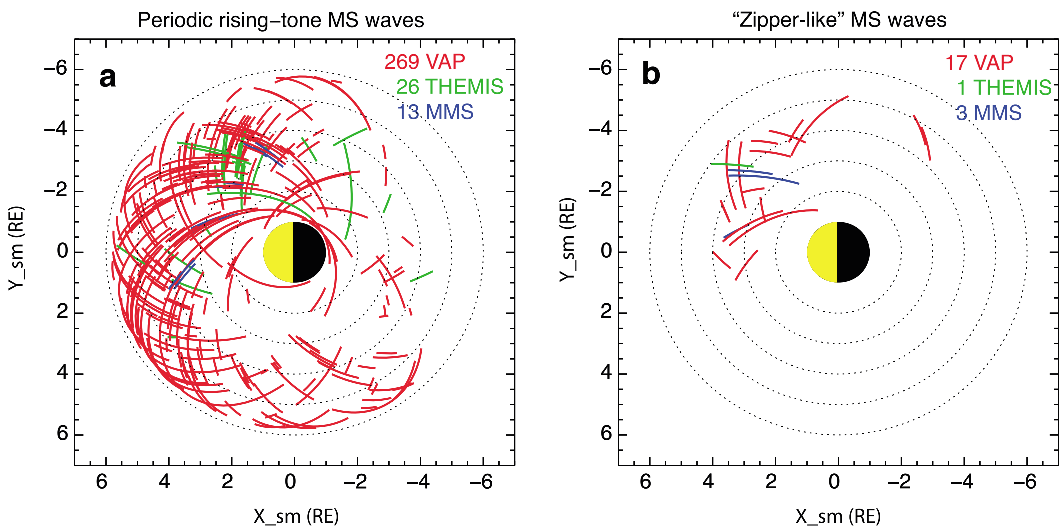

Figure 5. (a) Statistical spatial distributions of rising-tone MS waves, and (b) zipper-like MS waves based on observations by Van Allen Probes (red) and THEMIS (green) from September 2012 to April 2016 and observations by MMS satellites (blue) from April 2015 to April 2016. The number of events recorded by each spacecraft is labeled with the corresponding color.

by 1 order, a future work investigating the rising-tone MS waves, especially via multipoint simultaneous measurements, may reveal the mysterious characteristics of these waves such as the wave source and the periodicity variation along L shell.

5. Conclusions

This paper reports the discovery of a fascinating zipper-like MS wave using the MMS, the Van Allen Probes, and the THEMIS measurements. We presented three cases to illustrate the features of this new MS wave structure, and a statistical survey was performed to study their spatial distribution. The main conclusions are as follows:

1. Zipper-like MS waves are comprised of two-frequency-band periodic rising-tone emissions, which interleave together. In some cases, the wave intensity of the two bands differs significantly.
2. The periodicity of the two bands in a zipper-like MS wave remains the same while it varies in space and time. In case 2, a constant-frequency continuous MS wave developed into a discrete one with the same periodicity as the zipper-like MS waves, and an electrostatic emission was also found to have the same periodicity, suggesting that the two bands of the zipper-like MS waves probably originated from one single source intrinsically.
3. The zipper-like MS waves occur mostly above 10 f_{cp} and below f_{LHR}, distinct from ordinary continuous MS waves which have a statistical intensity peak below 10 f_{cp}.
4. The zipper-like MS waves are not modulated by ULF waves or plasma density fluctuation.
5. A total of 21 zipper-like MS waves were identified over the Van Allen Probes era, and they distribute mostly on the dawnside to noonside.

While the excitation or modulation mechanism of rising-tone MS waves still remains to be fully understood, it is clear from this study (and previous study [*Fu et al.*, 2014; *Boardsen et al.*, 2014]) that these waves are not related to ULF pulsations or density modulations. It is possible that there may still be an external driver that modulates the wave excitation, which has not been identified or observed yet, or that the periodicity of the MS waves arises due to an internal instability, analogous to what has been suggested for whistler mode chorus waves [e.g., *Bespalov et al.*, 2010; *Trakhtengerts*, 1998]. The observation of zipper-like MS waves exhibits additional complexity but may provide a new clue in understanding the causative mechanism of the modulation, which is important since periodic wave structures have been observed in a variety of waves [*Fu et al.*, 2014], including chorus [e.g., *Hayosh et al.*, 2014; *Němec et al.*, 2014; *Manninen et al.*, 2014] and EMIC waves [e.g., *Pickett et al.*, 2010; *Grison et al.*, 2013; *Sakaguchi et al.*, 2013], and they have been observed at other magnetized planets as well [e.g., *Menietti* et al., 2013]. Periodic emissions appear to be a universal plasma physical process and are still poorly understood. This study also demonstrates that the MMS spacecraft, although designed for investigation of magnetic reconnections in the boundary of Earth's magnetosphere, are robust in the study of electromagnetic waves in the radiation belts.

Acknowledgments
J.L. and J.B. would like to acknowledge NASA grants NNX13AI61G and NNX14AN85G. W.L., Q.M., and R.M.T. acknowledge EMFISIS subaward 1001057397:01, the ECT subaward 13–041, and NSF Geospace Environment Modeling grant AGS-1405054. This work is also supported by JHU/APL contracts 967399 and 921647 under NASA's prime contract NAS5-01072. The RBSPICE instrument is supported by JHU/APL subcontract 937836 to the New Jersey Institute of Technology under NASA prime contract NAS5-01072. The work at the University of Minnesota was supported by JHU/APL contract UMN 922613 under NASA contract JHU/APL NAS5-01072. We thank the entire MMS team and instrument leads for data access and support. The French involvement (SCM instruments) on THEMIS and MMS is supported by CNES, CNRS-INSIS, and CNRS-INSU. We acknowledge the Van Allen Probes data from the EMFISIS instrument obtained from https://emfisis.physics.uiowa.edu/data/index, the EFW instrument data obtained from http://www.space.umn.edu/missions/rbspefw-home-university-of-minnesota/, the ECT instrument data obtained from https://www.rbsp-ect.lanl.gov/, and the RBSPICE data obtained from http://rbspice.ftecs.com/. We acknowledge the MMS data obtained from https://lasp.colorado.edu/mms/sdc/public/ and the THEMIS data obtained from http://themis.ssl.berkeley.edu/index.shtml. We also thank the World Data Center for Geomagnetism, Kyoto for providing *SYM*-H and AE indexes (http://wdc.kugi.kyoto-u.ac.jp/aeasy/index.html). We thank V. Angelopoulos (University of California, Los Angeles), S. Wellenzohn (Space Research Institute, Austrian Academy of Sciences), and L. J. Lanzerotti (New Jersey Institute of Technology) for their great contributions.

References

Andriopoulou, M., R. Nakamura, K. Torkar, W. Baumjohann, and B. Hoelzl (2015), Deriving plasma densities in tenuous plasma regions, with the spacecraft potential under active control, *J. Geophys. Res. Space Physics*, *120*, 9594–9616, doi:10.1002/2015JA021472.

Andriopoulou, M., R. Nakamura, K. Torkar, W. Baumjohann, R. B. Torbert, P.-A. Lindqvist, Y. V. Khotyaintsev, J. Dorelli, J. L. Burch, and C. T. Russell (2016), Study of the spacecraft potential under active control and plasma density estimates during the MMS commissioning phase, *Geophys. Res. Lett.*, *43*, 4858–4864, doi:10.1002/2016GL068529.

Angelopoulos, V. (2008), The THEMIS Mission, *Space Sci. Rev.*, *141*(1–4), 5–34, doi:10.1007/s11214-008-9336-1.

Balikhin, M. A., Y. Y. Shprits, S. N. Walker, L. Chen, N. Cornilleau-Wehrlin, I. Dandouras, O. Santolik, C. Carr, K. H. Yearby, and B. Weiss (2015), Observations of discrete harmonics emerging from equatorial noise, *Nat. Commun.*, *6*, 7703, doi:10.1038/ncomms8703.

Bespalov, P. A., M. Parrot, and J. Manninen (2010), Short-period VLF emissions as solitary envelope waves in a magnetospheric plasma maser, *J. Atmos. Sol. Terr. Phys.*, *72*(17), 1275–1281, doi:10.1016/j.jastp.2010.09.001.

Boardsen, S. A., G. B. Hospodarsky, C. A. Kletzing, R. F. Pfaff, W. S. Kurth, J. R. Wygant, and E. A. MacDonald (2014), Van Allen Probe observations of periodic rising frequencies of the fast magnetosonic mode, *Geophys. Res. Lett.*, *41*, 8161–8168, doi:10.1002/2014GL062020.

Boardsen, S. A., et al. (2016), Survey of the frequency dependent latitudinal distribution of the fast magnetosonic wave mode from Van Allen Probes Electric and Magnetic Field Instrument and Integrated Science waveform receiver plasma wave analysis, *J. Geophys. Res. Space Physics*, *121*, 2902–2921, doi:10.1002/2015JA021844.

Bonnell, J. W., F. S. Mozer, G. T. Delory, A. J. Hull, R. E. Ergun, C. M. Cully, V. Angelopoulos, and P. R. Harvey (2008), The Electric Field Instrument (EFI) for THEMIS, *Space Sci. Rev.*, *141*, 303–341, doi:10.1007/s11214-008-9469-2.

Burch, J. L., T. E. Moore, R. B. Torbert, and B. L. Giles (2015), Magnetospheric multiscale overview and science objectives, *Space Sci. Rev.*, *199*, 5–21, doi:10.1007/s11214-015-0164-9.

Chen, L. (2015), Wave normal angle and frequency characteristics of magnetosonic wave linear instability, *Geophys. Res. Lett.*, *42*, 4709–4715, doi:10.1002/2015GL064237.

Chen, L., and R. M. Thorne (2012), Perpendicular propagation of magnetosonic waves, *Geophys. Res. Lett.*, *39*, L14102, doi:10.1029/2012GL052485.

Chen, L., R. M. Thorne, V. K. Jordanova, and R. B. Horne (2010), Global simulation of magnetosonic wave instability in the storm time magnetosphere, *J. Geophys. Res.*, *115*, A11222, doi:10.1029/2010JA015707.

Chen, L., R. M. Thorne, V. K. Jordanova, M. F. Thomsen, and R. B. Horne (2011), Magnetosonic wave instability analysis for proton ring distributions observed by the LANL magnetospheric plasma analyzer, *J. Geophys. Res.*, *116*, A03223, doi:10.1029/2010JA016068.

Chen, L., J. Sun, Q. Lu, X. Gao, Z. Xia, and Z. Zhima (2016), Generation of magnetosonic waves over a continuous spectrum, *J. Geophys. Res. Space Physics*, *121*, 1137–1147, doi:10.1002/2015JA022089.

Ergun, R. E., et al. (2014), The axial double probe and fields signal processing for the MMS mission, *Space Sci. Rev.*, *199*(1), 167–188, doi:10.1007/s11214-014-0115-x.

Fu, H. S., J. Tu, P. Song, J. B. Cao, B. W. Reinisch, and B. Yang (2010a), The nightside-to-dayside evolution of the inner magnetosphere: Imager for Magnetopause-to-Aurora Global Exploration Radio Plasma Imager observations, *J. Geophys. Res.*, *115*, A04213, doi:10.1029/2009JA014668.

Fu, H. S., J. Tu, J. B. Cao, P. Song, B. W. Reinisch, D. L. Gallagher, and B. Yang (2010b), IMAGE and DMSP observations of a density trough inside the plasmasphere, *J. Geophys. Res.*, *115*, A07227, doi:10.1029/2009JA015104.

Fu, H. S., J. B. Cao, Z. Zhima, Y. V. Khotyaintsev, V. Angelopoulos, O. Santolík, Y. Omura, U. Taubenschuss, L. Chen, and S. Y. Huang (2014), First observation of rising-tone magnetosonic waves, *Geophys. Res. Lett.*, *41*, 7419–7426, doi:10.1002/2014GL061867.

Funsten, H. O., et al. (2013), Helium, Oxygen, Proton, and Electron (HOPE) mass spectrometer for the Radiation Belt Storm Probes Mission, *Space Sci. Rev.*, doi:10.1007/s11214-013-9968-7.

Fuselier, S. A., et al. (2016), Magnetospheric multiscale science mission profile and operations, *Space Sci. Rev.*, doi:10.1007/s11214-014-0087-x.

Grison, B., O. Santolk, N. Cornilleau-Wehrlin, A. Masson, M. J. Engebretson, J. S. Pickett, Y. Omura, P. Robert, and R. Nomura (2013), EMIC triggered chorus emissions in Cluster data, *J. Geophys. Res. Space Physics*, *118*, 1159–1169, doi:10.1002/jgra.50178.

Gurnett, D. A. (1976), Plasma wave interactions with energetic ions near the magnetic equator, *J. Geophys. Res.*, *81*, 2765–2770, doi:10.1029/JA081i016p02765.

Hayosh, M., F. Němec, O. Santolík, and M. Parrot (2014), Statistical investigation of VLF quasiperiodic emissions measured by the DEMETER spacecraft, *J. Geophys. Res. Space Physics*, *119*, 8063–8072, doi:10.1002/2013JA019731.

Horne, R. B., G. V. Wheeler, and H. S. C. K. Alleyne (2000), Proton and electron heating by radially propagating fast magnetosonic waves, *J. Geophys. Res.*, *105*, 27,597–27,610, doi:10.1029/2000JA000018.

Horne, R. B., R. M. Thorne, S. A. Glauert, N. P. Meredith, D. Pokhotelov, and O. Santolik (2007), Electron acceleration in the Van Allen radiation belts by fast magnetosonic waves, *Geophys. Res. Lett.*, *34*, L17107, doi:10.1029/2007GL030267.

Hrbáčková, Z., O. Santolík, F. Němec, E. Macúšová, and N. Cornilleau-Wehrlin (2015), Systematic analysis of occurrence of equatorial noise emissions using 10 years of data from the Cluster mission, *J. Geophys. Res. Space Physics*, *120*, 1007–1021, doi:10.1002/2014JA020268.

Kistler, L. M., et al. (2016), The source of O^+ in the storm time ring current, *J. Geophys. Res. Space Physics*, *121*, 5333–5349, doi:10.1002/2015JA022204.

Kletzing, C., et al. (2013), The electric and magnetic field instrument suite and integrated science (EMFISIS) on RBSP, *Space Sci. Rev.*, *179*, 127–181, doi:10.1007/s11214-013-9993-6.

Le Contel, O., et al. (2008), First results of the THEMIS Search Coil Magnetometers, *Space Sci. Rev.*, doi:10.1007/s11214-008-9371-y.

Le Contel, O., et al. (2014), The search-coil magnetometer for MMS, *Space Sci. Rev.*, *199*, 257–282, doi:10.1007/s11214-014-0096-9.

Li, J., et al. (2016a), Formation of energetic electron butterfly distributions by magnetosonic waves via Landau resonance, *Geophys. Res. Lett.*, *43*, 3009–3016, doi:10.1002/2016GL067853.

Li, J., et al. (2016b), Ultrarelativistic electron butterfly distributions created by parallel acceleration due to magnetosonic waves, *J. Geophys. Res. Space Physics*, *121*, 3212–3222, doi:10.1002/2016JA022370.

Lindqvist, P.-A., et al. (2016), The spin-plane double probe electric field instrument for MMS, *Space Sci. Rev.*, *199*(1), 137–165, doi:10.1007/s11214-014-0116-9.

Lybekk, B., A. Pedersen, S. Haaland, K. Svenes, A. N. Fazakerley, A. Masson, M. G. G. T. Taylor, and J.-G. Trotignon (2012), Solar cycle variations of the Cluster spacecraft potential and its use for electron density estimations, *J. Geophys. Res.*, *117*, A01217, doi:10.1029/2011JA016969.

Ma, Q., W. Li, R. M. Thorne, and V. Angelopoulos (2013), Global distribution of equatorial magnetosonic waves observed by THEMIS, *Geophys. Res. Lett.*, *40*, 1895–1901, doi:10.1002/grl.50434.

Ma, Q., W. Li, L. Chen, R. M. Thorne, and V. Angelopoulos (2014a), Magnetosonic wave excitation by ion ring distribution in the Earth's inner magnetosphere, *J. Geophys. Res. Space Physics*, *119*, 844–852, doi:10.1002/2013JA019591.

Ma, Q., W. Li, L. Chen, R. M. Thorne, C. A. Kletzing, W. S. Kurth, G. B. Hospodarsky, G. D. Reeves, M. G. Henderson, and H. E. Spence (2014b), The trapping of equatorial magnetosonic waves in the Earth's outer plasmasphere, *Geophys. Res. Lett.*, *41*, 6307–6313, doi:10.1002/2014GL061414.

Ma, Q., W. Li, R. M. Thorne, J. Bortnik, C. A. Kletzing, W. S. Kurth, and G. B. Hospodarsky (2015), Electron scattering by magnetosonic waves in the inner magnetosphere, *J. Geophys. Res. Space Physics*, *121*, 274–285, doi:10.1002/2015JA021992.

Maldonado, A. A., L. Chen, S. G. Claudepierre, J. Bortnik, R. M. Thorne, and H. Spence (2016), Electron butterfly distribution modulation by magnetosonic waves, *Geophys. Res. Lett.*, *43*, 3051–3059, doi:10.1002/2016GL068161.

Manninen, J., A. G. Demekhov, E. E. Titova, A. E. Kozlovsky, and D. L. Pasmanik (2014), Quasiperiodic VLF emissions with short-period modulation and their relationship to whistlers: A case study, *J. Geophys. Res. Space Physics*, *119*, 3544–3557, doi:10.1002/2013JA019743.

Mauk, B. H., N. J. Fox, S. G. Kanekal, R. L. Kessel, D. G. Sibeck, and A. Ukhorskiy (2013), Science objectives and rationale for the radiation belt storm probes mission, *Space Sci. Rev.*, *179*, 3–27, doi:10.1007/s11214-012-9908-y.

Menietti, J. D., P. Schippers, Y. Katoh, J. S. Leisner, G. B. Hospodarsky, D. A. Gurnett, and O. Santolik (2013), Saturn chorus intensity variations, *J. Geophys. Res. Space Physics*, *118*, 5592–5602, doi:10.1002/jgra.50529.

Meredith, N. P., R. B. Horne, and R. R. Anderson (2008), Survey of magnetosonic waves and proton ring distributions in the Earth's inner magnetosphere, *J. Geophys. Res.*, *113*, A06213, doi:10.1029/2007JA012975.

Mitchell, D., et al. (2013), Radiation Belt Storm Probes Ion Composition Experiment (RBSPICE), *Space Sci. Rev.*, *179*(1–4), 263–308, doi:10.1007/s11214-013-9965-x.

Němec, F., O. Santolík, J. S. Pickett, Z. Hrbáčková, and N. Cornilleau-Wehrlin (2013), Azimuthal directions of equatorial noise propagation determined using 10 years of data from the Cluster spacecraft, *J. Geophys. Res. Space Physics*, *118*, 7160–7169, doi:10.1002/2013JA019373.

Němec, F., J. S. Pickett, and O. Santolík (2014), Multispacecraft Cluster observations of quasiperiodic emissions close to the geomagnetic equator, *J. Geophys. Res. Space Physics*, *119*, 9101–9112, doi:10.1002/2014JA020321.

Němec, F., O. Santolík, Z. Hrbáčková, J. S. Pickett, and N. Cornilleau-Wehrlin (2015), Equatorial noise emissions with quasiperiodic modulation of wave intensity, *J. Geophys. Res. Space Physics*, *120*, 2649–2661, doi:10.1002/2014JA020816.

Pedersen, A., et al. (2008), Electron density estimations derived from spacecraft potential measurements on Cluster in tenuous plasma regions, *J. Geophys. Res.*, *113*, A07S33, doi:10.1029/2007JA012636.

Perraut, S., A. Roux, P. Robert, R. Gendrin, J.-A. Sauvaud, J.-M. Bosqued, G. Kremser, and A. Korth (1982), A systematic study of ULF waves Above F_{H+} from GEOS 1 and 2 measurements and their relationships with proton ring distributions, *J. Geophys. Res.*, *87*, 6219–6236, doi:10.1029/JA087iA08p06219.

Pickett, J. S., et al. (2010), Cluster observations of EMIC triggered emissions in association with Pc1 waves near Earth's plasmapause, *Geophys. Res. Lett.*, *37*, L09104, doi:10.1029/2010GL042648.

Roux, A., O. Le Contel, C. Coillot, A. Bouabdellah, B. de la Porte, D. Alison, S. Ruocco, and M. C. Vassal (2008), The search coil magnetometer for THEMIS, *Space Sci. Rev.*, *141*, 265–275, doi:10.1007/s11214-008-9371-y.

Russell, C. T., R. E. Holzer, and E. J. Smith (1970), OGO 3 observations of ELF noise in the magnetosphere: 2. The nature of the equatorial noise, *J. Geophys. Res.*, *75*, 755–768, doi:10.1029/JA075i004p00755.

Russell, C. T., et al. (2014), The Magnetospheric Multiscale magnetometers, *Space Sci. Rev.*, doi:10.1007/s11214-014-0057-3.

Sakaguchi, K., Y. Kasahara, M. Shoji, Y. Omura, Y. Miyoshi, T. Nagatsuma, A. Kumamoto, and A. Matsuoka (2013), Akebono observations of EMIC waves in the slot region of the radiation belts, *Geophys. Res. Lett.*, *40*, 5587–5591, doi:10.1002/2013GL058258.

Santolík, O., Pickett, J. S., Gurnett, D. A., Maksimovic, M., and Cornilleau-Wehrlin, N. (2002), Spatiotemporal variability and propagation of equatorial noise observed by Cluster, *J. Geophys. Res. 107*(A12), 1495, doi:10.1029/2001JA009159.

Torbert, R. B., et al. (2014), The FIELDS instrument suite on MMS: Scientific objectives, measurements, and data products, *Space Sci. Rev.*, *199*, 105–135, doi:10.1007/s11214-014-0109-8.

Torkar, K., R. Nakamura, M. Tajmar, C. Scharlemann, H. Jeszenszky, G. Laky, G. Fremuth, C. P. Escoubet, and K. Svenes (2014), Active spacecraft potential control investigation, *Space Sci. Rev.*, *199*, 515–544, doi:10.1007/s11214-014-0049-3.

Trakhtengerts, V. Y. (1998), A generation mechanism for chorus emission, *Ann. Geophys.*, *17*, 95, doi:10.1007/s00585-999-0095-4.

Wygant, J. R., et al. (2013), The electric field and waves instrument on the Radiation Belt Storm Probes mission, *Space Sci. Rev.*, *179*, 183–220, doi:10.1007/s11214-013-0013-7.